How does Bottom Friction affect Tsunami waves?

Jack Britton
Supervisor: Dr. Omar Lakkis

Works presented as a Junior Research Associate.

School Of Mathematical and Physicial Sciences
University of Sussex
GB
September 2020

Contents

1 Poster

This contains parts of the final poster, and parts that were cut out due to lack of space.

1.1 Elements

1.1.1 Title

How does Bottom Friction affect Tsunami waves?

1.1.2 Contributors

Jack Britton, Dr. Omar Lakkis. School of Mathematical and Physical Sciences.

1.1.3 Introduction

Tsunami waves experience bottom friction as water moves across a foreign object - such as sand, concrete, or tree roots. This force resists the motion of the wave, altering its characteristics. One quantification of bottom friction is Manning's friction coefficient, also known as Manning's n, or n. In this project, simulations of the Chile 2010 tsunami – varying only by a change in Manning's n – were ran, and several characteristics of the waves were measured, to observe the effect Manning's n had on wave characteristics.

1.1.4 Motivation

Simulations provide insights into tsunami behaviour and impact. They can be used in: preparation - to better situate vital infrustructure and evacuation routes; and emergencies - to issue warnings and evacuations [1]. On the 27th of February, 2010 – an 8.8 Mw earthquake occurred on the coast of Chile, triggering a tsunami. Approximately 500 lives were lost, and between 200 000 to 400 000 houses were severly damaged or destroyed [2], [3].

1.1.5 Methodology

A pre-existing, basic model of the 2010 Chile tsunami from the CLAWPACK software was used. This was subsequently modified to produce comparitive and descriptive graphs and animations. The adapted software is available on github at see-on/apps.

The tsunami was modelled on a system of hyperbolic partial differential equations (PDEs) with source terms, known as shallow water equations (Eq. 1). The PDEs were discretised - converting them into Riemann problems - using the Corner Transport Upwind method plus MC limiters - with single waves passing through 75-100% of one grid cell only. Godunov's splitting method was employed to solve the homogenous form of each Riemann problem, and the solution provided initial values for the inhomogeneous Riemann problem to be approximated via the Lax-Wendroff solver. The friction coefficient was applied uniformly to the entire sea bed.

Gauges on artificial buoys, and one real buoy: DART buoy 32412, recorded data of various wave characteristics. Gauges which measured velocity, height, and discharge, were on buoys modelled using the Eulerian specification of the fliud field. Displacement was measured using gauges on buoys modelled on the Lagrangian specification of the fluid field. The Constitucion buoy - numbered '6' (Fig. x) - was located 6km west of the Constitucion coast, as the program read the sea depth as zero at any point closer to land than this.

1.1.6 Results

Results The effect of the Manning's n value was proportionally insignificant in the westward wave velocity recording by the epicentre buoy (Fig. x). The northward wave displayed distinct curves after 1.5 h, with n affecting the velocity of the wave by over 10 km/h. Displacement of the buoy on the Constitucion coast (Fig. x) varied by over 700 m in the east-west direction. Between simulated Manning's n values of 0.094 and 0.172 (a range of 0.078), the displacement of the buoy differed by around 50 m. Between n = 0.06 and 0.08 (a range of 0.02), the displacement differed by over 200 m. Buoy 32412 (Fig. x) was simulated using a very large range of Manning's n values. The gauge registered the maximum difference in sea surface elevation to be less than 5 cm – occuring between n = 0, and n= 1.8. In both directions, the discharge at buoy 123 (Fig. x) spiked at approx 6.75

h only on the simulation with manning's n value 0.094. Most values followed a general curve, but the largest and smallest value: 0.172 and 0.02 respectively – were also distinct from this.

1.1.7 Tables

Manning's n table.

	Kotani et. al. (1998)	Koshimura et. al. (2009) based on Petryk and Bosmajian (1975)	Yanagisawa et. al. (2009)
Coastal & riverine areas	0.025	0.025	0.025
Farmland Bare ground and grass ◇	0.02	0.02	◇ 0.02
Forest Mangrove ⋆ Barringtonia, Casuarinas, Catappa †	0.03	0.03	⋆ 0.04 † 0.05
Low-density urban	0.04	0.053	
Medium-density urban Buildings •	0.06	0.094	• 0.06
High-density urban	0.08	0.172	

Table 1: Manning's n friction coefficient on a variety of terrain, adapted from Bricker et. al. (2015).

1.1.8 Equation

Shallow water equations

$$
\begin{aligned}
h_t + (hu)_x + (hv)_y &= 0 \\
(hu)_t + (hu^2 + \tfrac{1}{2}gh^2)_x + (huv)_y &= -ghB_x - \gamma hu \\
(hv)_t + (huv)_x + (hv^2 + \tfrac{1}{2}gh^2)_y &= -ghB_y - \gamma hv \\
\gamma &\coloneqq gn^2 h^{-\frac{7}{3}} \sqrt{(hu)^2 + (hv)^2}
\end{aligned}
$$

Equation 1: The shallow water equations, where h is the water column height, t is the time-step, u and v are depth-averaged velocities in the east-west and north-south directions respectively, g is the gravitational constant, $B(x, y, t)$ is bathymetry data, and n is Manning's n friction coefficient.

1.1.9 Figures

1

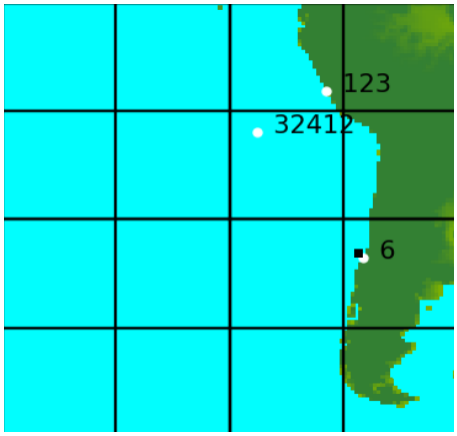

Figure 1: Map of the simulated region. White dots represent simulated buoys. The black square represents the epicentre of the earthquake.

2

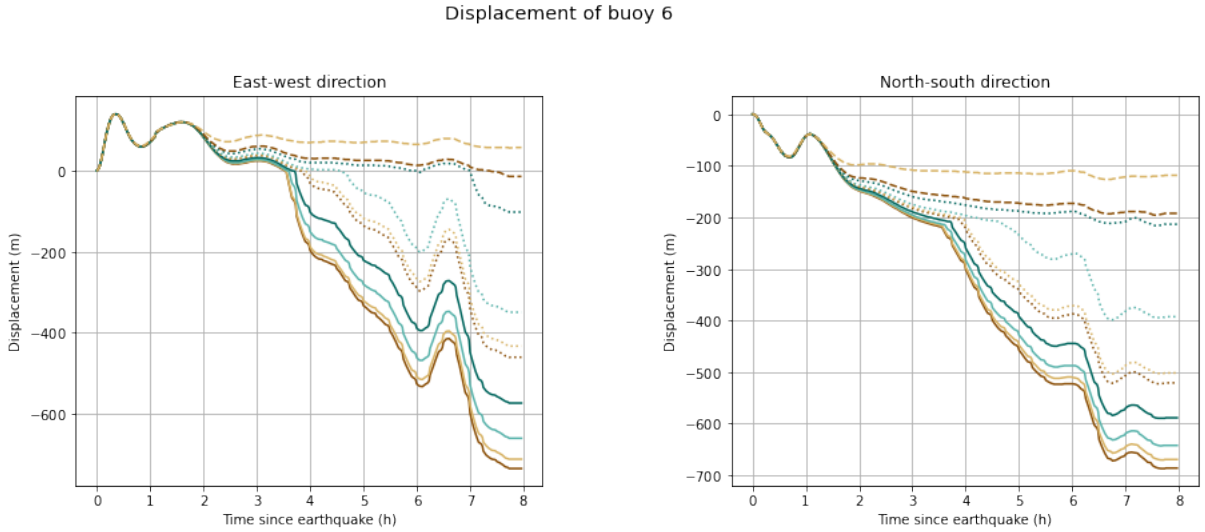
Displacement of buoy 6
East-west direction
North-south direction
Displacement (m)
Time since earthquake (h)

∞

(a)

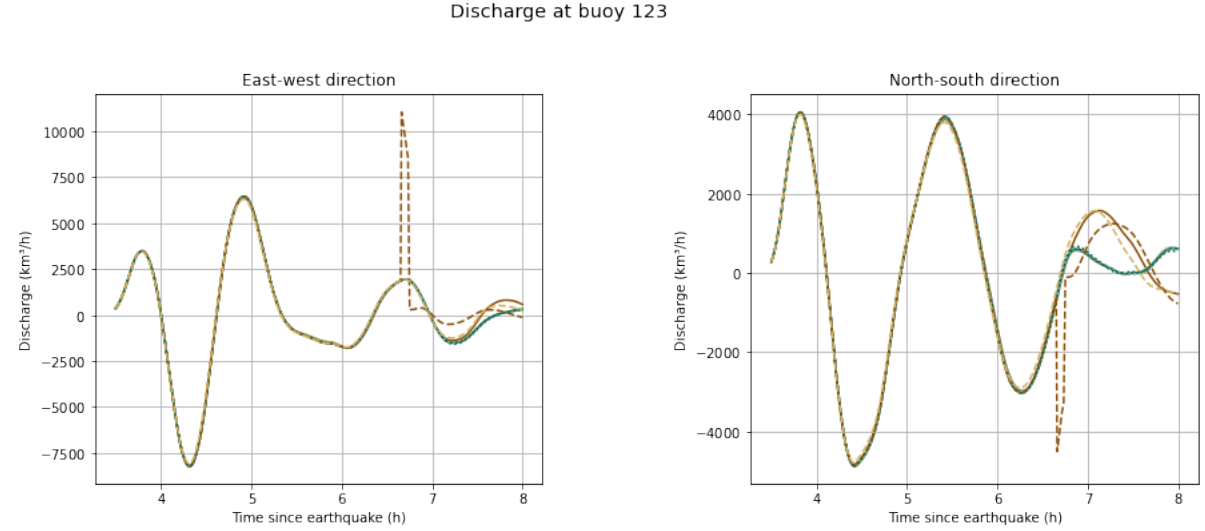
Discharge at buoy 123
East-west direction
North-south direction
Discharge (km³/h)
Time since earthquake (h)

(b)

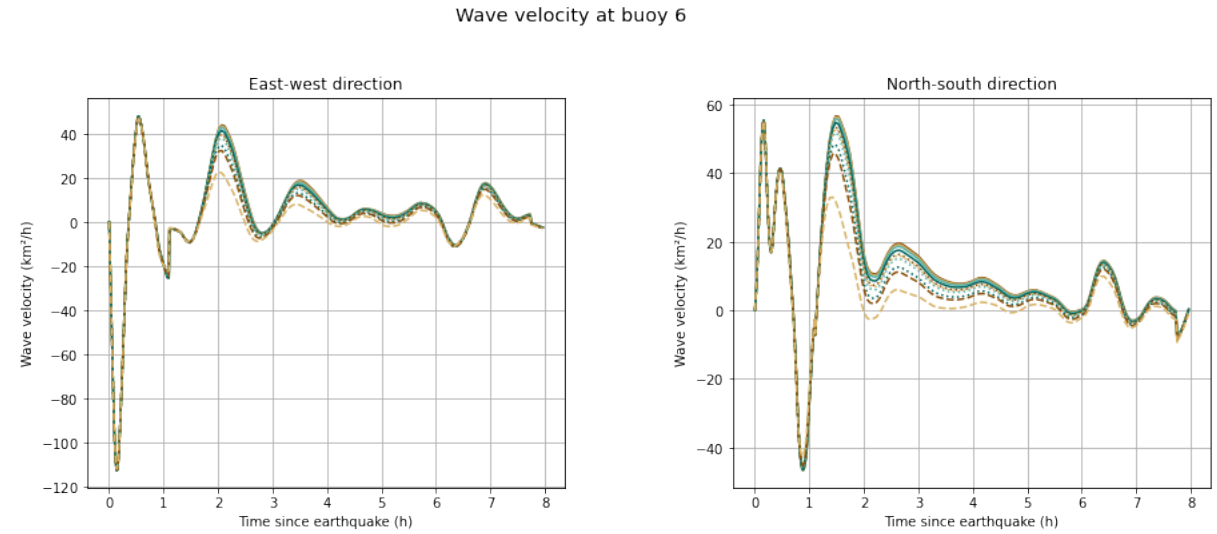

(c)

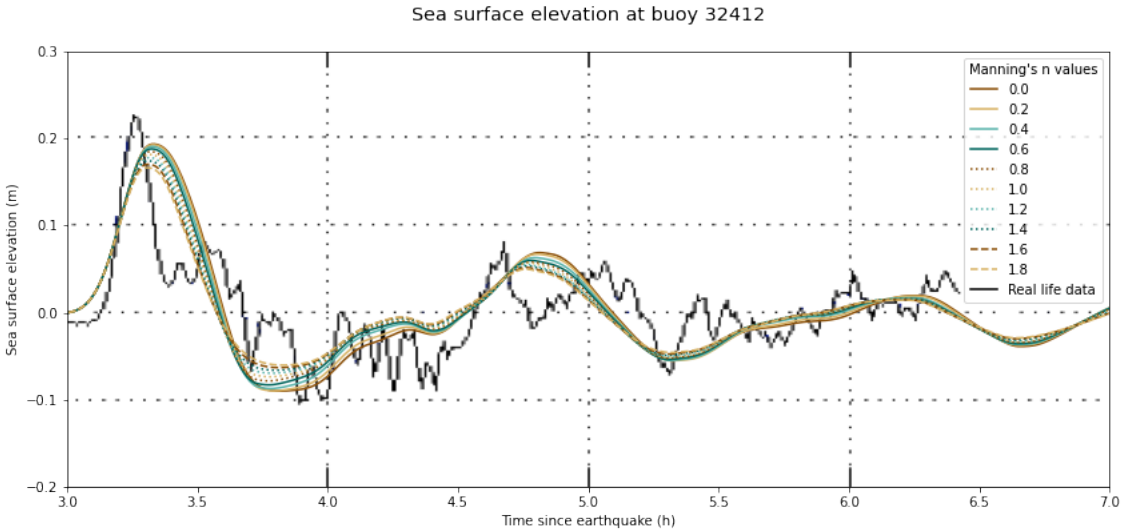

(d)

Figure 2: Measurements of wave characteristics, with modification of Manning's n value listed in Table 1 unless described otherwise on the graph. For east-west measurements: east is positive, west is negative; and for north-south: north is positive, south is negative.

2 Understanding

This document was cascade understanding from the core element of my JRA - Manning's coefficient of roughness, to the combination of elements that results in a simulation.

2.1 Manning's equation and friction coefficient

In a tsunami, water flows in a non-steady manner - that is, it the flow of the water changes with time. Manning's equation is based off steady flow, and as such, use as an estimation for the friction slope specifically in a tsunami is inaccurate [4]. However, adapted versions of Manning's equation which do have a base in unsteady flow are used to model tsunamis, so we detail the original here as a core base of understanding.

2.1.1 Manning's friction coefficient

$$n = R_h^{1/6} \left(\frac{f}{8g} \right)^{1/2}$$

Manning's friction coefficient (also known as Manning's n) is a numerical representation of the bottom friction applied to the flow from a foreign surface [5]. It is a function of the following elements:

- (R_h/m) is the hydraulic radius. In modelling channel flow, it is typical to use the definition [6, ch. 14.4]:
$$R_h = \frac{A}{P_w}$$
where (A/m^2) is the cross sectional area, and (P_w/m) is the wetted perimeter. Thus the hydraulic radius is a ratio of A to P_w , measured in meters.
- f is the (Darcy) friction factor, which is evaluated by several fluid and environmental characteristics. It is used in the evaluation of the friction slope function.
- $(g/[\mathrm{m/s}^2])$ is the gravitational constant.

2.1.2 Manning's equation

$$S_f = \frac{U^2 n^2}{R_h^{4/3}}$$

Where:

- $(U/[\mathrm{m/s}])$ is the average velocity
- $(S_f/[\mathrm{m/m}])$ is the friction slope, which describes the rate of energy loss along a length of channel [7].

2.2 Conservation laws/ equations

The conservation laws are hyperbolic partial differential equations which describe the conservation of physical quantities. For example, the conservation-of-momentum equation describes the manner in which momentum is conserved in a system, not lost through entropy.

2.3 Momentum equation for hydraulic routing

$$\frac{\partial(\bar{\rho})UA}{\partial t} + \frac{\partial(\bar{\rho}\beta U^2 A)}{\partial x} - \bar{\rho}gA(S_0 - \frac{\partial H}{\partial x} - S_f) = 0$$

The conservation-of-momentum equation for hydraulic routing takes, as one of its arguments, S_f, the friction slope, which arises initially as a notation change. [6, ch. 14.3.2].

2.4 Shallow water equations

The shallow water equations are a system of conservation laws(*Not possible to be balance laws?*). Together, these laws describe the behaviour of shallow water waves [8]. A tsunami behaves as shallow water waves - and are therefore modelled using the shallow water equations [9]. The set of equations to be solved in this model were the following:

$$\begin{aligned}
h_t + (hu)_x + (hv)_y &= 0 \\
(hu)_t + (hu^2 + \tfrac{1}{2}gh^2)_x + (huv)_y &= -ghB_x - \gamma hu \\
(hv)_t + (huv)_x + (hv^2 + \tfrac{1}{2}gh^2)_y &= -ghB_y - \gamma hv \\
\gamma &\coloneqq gn^2 h^{-\frac{7}{3}}\sqrt{(hu)^2 + (hv)^2}
\end{aligned}$$

h is the water column height [10], t is the time-step, u and v are depth-averaged velocities in the east-west and north-south directions respectively, $B(x, y, t)$ is bathymetry data, g is the gravitational constant [11], n is Manning's n friction coefficient [12], [13, ch. 2.1], [14].

2.5 Numerical discretisation method

The curves plotted by the shallow water equations are continuous, which is incomprehensible computationally, therefore, the PDEs must be discretised to be modelled. This discretisation is performed using a finite volume method, which sections the spatial domain into grid cells (aka finite volumes), and track the approximation of the integral of the flux over each of these intervals. At each time step, the value of the curve at each point is updated using the approximations of the flux through the endpoints of the interval. This most often leads to a non smooth curve between two adjacent cells. This sets up a Riemann problem in between each pair of cells/ This transforms the continuous problem into many discrete, Riemann problems [15, p. 64]. In this model, the finite volume method used was the Corner Transport Upwind method.

2.6 Courant number

The Courant-Friedrichs-Lewy (CFL) condition is a necessary stability condition for a numerical method [15, p. 69]. To satisfy the condition, there must be set a restriction of the permissible time step: requiring that no wave can pass through more than one grid cell in a single time step [16, ch. 2.1]. In this model, this description reflects the 'Maximum Courant number' parameter. Restricting the the wave movement to more 75% of the grid cell is what the 'Desired Courant number' does.

Hence, in this model, the wave must pass through between 75% and 100% of one grid cell in a single time step.

2.7 Riemann problems

Riemann problems are '(a) hyperbolic partial differential equation(s) (PDE(s)) with initial data consisting of two constant states separated by a discontinuity' [16, ch. 1.1]. The initial data would look something like this.

$$u = \begin{cases} 0 & x_i < 0 \\ 1 & x_i > 0 \end{cases}$$

The hyperbolic PDEs in our case are the shallow water equations.

2.8 Riemann solvers

Lax-Wendroff is Godunov based Riemann solver. In this situation, the Corner Transport Upwind method is used, creating pairs of Riemann problems. These pairs are described generally using Godunov's scheme, into PDEs that can be approximately solved using a Godunov-based Riemann solver. Exact solutions to the Riemann problem are often costly to compute, which is why approximate Riemann solvers are often used [15, p. 264].

2.9 Fractional-step method

Often, conservation laws include a source term, making them more difficult to solve due to their lack of homogeneity. With a source term, these laws are usually instead referred to as balance laws [15, p. 375]. In this description, we will use the term 'conservation law' to refer to the homogeneous form of the 'balance law'. A fractional-step method is used in two steps. First, solve the conservation law(s). Second, The solution from the first step is used as the initial condition for the IVP of the balance law(s), which is to be solved using a Riemann solver, to produce an approximate solution to the balance law(s) [17]. *If the shallow water equations are balance laws, are they still balance laws when applying Godunov's scheme? If so, is this the method in which they are turned into a solvable form for the Riemann Solver?*

2.10 F-waves

Clawpack site says using this algorithm, the Riemann solver returns F-waves instead of regular waves. How does it do that?

2.11 Limiters

The flux equation, given by the CTU method, includes a correction term. A limiter adjusts the magnitude of the correction term dependent on the behaviour of the solution [15, p. 103]. This has the effect of tailoring the approximation produced by the CTU method to the behaviour of the PDE in its exact form.

3 Simulation

3.1 Sample Manning's values to simulate

	Kotani et. al. (1998)	Koshimura et. al. (2009) based on Petryk and Bosmajian (1975)	Yanagisawa et. al. (2009)
Coastal & riverine areas	0.025	0.025	0.025
Farmland Bare ground and grass ◇	0.02	0.02	◇ 0.02
Forest Mangrove ⋆ Barringtonia, Casuarinas, Catappa †	0.03	0.03	⋆ 0.04 † 0.05
Low-density urban	0.04	0.053	
Medium-density urban Buildings •	0.06	0.094	• 0.06
High-density urban	0.08	0.172	

Kotani et. al. (1998) & Koshimura et. al. (2009) courtesy of Bricker et. al. (2015). Urban environments of Koshimura et. al. (2009) characterised by flow depth of 2 m, a drag coefficient of 1.5, and an average house width of 10 m. Low-density housing is assumed to have an occupancy ratio of 10%, medium-density 30%, and high-density 60%. [4]. Yanagisawa et. al. (2009) values based at Pakarang Cape, Thailand. (Other) element refers to 'Vegetation other than grass', citing as an example Latief and Hadi (2007), who note species of the Genus Barringtonia, Casuarinas, and Catappa [18], [19].

3.2 Parameters

The simulation parameters are those preset for this notebook as of , some of which being the following [20], [21] (in order of appearance in the setrun.py file) :

Desired Courant number	0.75
Maximum Courant number	1.0
Riemann Solver	Lax-Wendroff (2^{nd} order)
Wave propagation method	Corner Transport Upwind plus second order correction terms [22]
Number of waves in Riemann solution	3
Limiter (for all waves)	MC
Wave propagation algorithm	F-waves [23]
Fractional-step method	Godunov (1^{st} order)
Coriolis force included in momentum equations	False
Friction depth	1E6

The simulation does not account for inundation, and the land border as given by Google Maps is not the same as the land border of the model. Neither does the model include (parameterise land for) islands in the South Pacific Ocean, only continental South America.

References

[1] *NOAA Center for Tsunami Research - Tsunami Modeling and Research*. [Online; accessed 20. Sep. 2020]. May 2018. URL: https://nctr.pmel.noaa.gov/model.html.

[2] OCHA. *Chile: Earthquake Situation Report*. Tech. rep. 6. [Online; accessed 20. Sep. 2020]. United Nations, Mar. 2010. URL: https://reliefweb.int/report/chile/chile-earthquake-situation-report-6.

[3] ECLAC, ed. *The Chilean earthquake of 27 February 2010 an overview*. Mar. 2010. URL: https://www.cepal.org/en/publications/3161-chilean-earthquake-27-february-2010-overview.

[4] Jeremy D. Bricker et al. "On the Need for Larger Manning's Roughness Coefficients in Depth-Integrated Tsunami Inundation Models". In: *Coastal Eng. J.* 57.02 (Apr. 2015), p. 1550005. ISSN: 0578-5634. DOI: 10.1142/S0578563415500059.

[5] *Manning's Equation*. [Online; accessed 25. Sep. 2020]. Feb. 2006. URL: http://www.fsl.orst.edu/geowater/FX3/help/8_Hydraulic_Reference/Manning_s_Equation.htm.

[6] William G. Gray and Genetha A. Gray. "Introduction to Environmental Modeling". In: *Higher Education from Cambridge University Press* (Dec. 2016). DOI: 10.1017/9781316422021.

[7] Thomas M. Walski and Inc Haestad Methods. *Computer Applications in Hydraulic Engineering: Connecting Theory to Practice, Volume 1*. Haestad Press, 2002, p. 7. ISBN: 978-097141414-3.

[8] Qiqi Wang. *Systems of conservation laws the shallow water equations.* [Online; accessed 21. Sep. 2020]. Dec. 2018. URL: https://www.youtube.com/watch?v=YyknI_38xkE.

[9] *How do tsunamis differ from other water waves?* [Online; accessed 21. Sep. 2020]. May 1996. URL: https://earthweb.ess.washington.edu/tsunami/general/physics/characteristics.html.

[10] *Riemann Solver Package - Clawpack 5.7.x documentation.* [Online; accessed 23. Sep. 2020]. Sept. 2020. URL: https://www.clawpack.org/pyclaw/rp.html?highlight=height#shallow-water-equations.

[11] clawpack. *riemann.* [Online; accessed 23. Sep. 2020]. Sept. 2020. URL: https://github.com/clawpack/riemann/blob/master/src/rpn2_geoclaw.f.

[12] *Manning friction term - Clawpack 5.7.x documentation.* [Online; accessed 23. Sep. 2020]. Sept. 2020. URL: https://www.clawpack.org/manning.html?highlight=manning#manning-friction-term.

[13] Frank I. González et al. "Validation of the GeoClaw Model". In: *NTHMP MMS Tsunami Inundation Model Validation Workshop. Validation of the GeoClaw Model.* [Online; accessed 23. Sep. 2020]. 2011. URL: https://depts.washington.edu/clawpack/links/nthmp-benchmarks/geoclaw-results.pdf.

[14] clawitzer. *apps.* [Online; accessed 23. Sep. 2020], section : SOURCES. Sept. 2020. URL: https://github.com/clawitzer/apps/blob/master/notebooks/geoclaw/chile2010b/Makefile.

[15] Randall J. LeVeque and J. Leveque Randall. *Finite Volume Methods for Hyperbolic Problems.* Cambridge University Press, Aug. 2002. ISBN: 978-052100924-9.

[16] D. I. Ketcheson, R. J. LeVeque, and M. J. Razo. *Riemann Problems and Jupyter Solutions.* Society for Industrial and Applied Mathematics, 2020. ISBN: 978-161197621-2. URL: https://www.clawpack.org/riemann_book/html/Index.html.

[17] Dongyang Kuang and Long Lee. "A conservation formulation and a numerical algorithm for the double-gyre nonlinear shallow-water model". In: *arXiv* (Mar. 2014). eprint: 1403.0140. URL: https://arxiv.org/abs/1403.0140v3.

[18] Hideaki Yanagisawa et al. "The reduction effects of mangrove forest on a tsunami based on field surveys at Pakarang Cape, Thailand and numerical analysis". In: *Estuarine Coastal Shelf Sci.* 81.1 (Jan. 2009), pp. 27–37. ISSN: 0272-7714. DOI: 10.1016/j.ecss.2008.10.001.

[19] Hamzah Latief and Sahwan Hadi. "Thematic paper: The role of forests and trees in protecting coastal areas against tsunamis". In: (Jan. 2007). URL: https://www.researchgate.net/publication/271194016_Thematic_paper_The_role_of_forests_and_trees_in_protecting_coastal_areas_against_tsunamis.

[20] *Specifying classic run-time parameters in setrun.py - Clawpack 5.7.x documentation.* [Online; accessed 14. Sep. 2020]. Sept. 2020. URL: https://www.clawpack.org/setrun.html#run-time-parameters.

[21] *Specifying GeoClaw parameters in setrun.py - Clawpack 5.7.x documentation.* [Online; accessed 14. Sep. 2020]. Sept. 2020. URL: https://www.clawpack.org/setrun_geoclaw.html#general-geo-parameters.

[22] Donna Calhoun. *Wave propagation algorithms in two dimensions, adaptive refinement and well-balancing*. Lecture. Jan. 2013. URL: https://www.bu.edu/pasi-tsunami/files/2013/01/lecture3_DAC.pdf.

[23] D. Bale et al. "A wave-propagation method for conservation laws and balance laws with spatially varying flux functions". In: *SIAM J. Sci. Comput.* 24 (2002), pp. 955–978. DOI: 10.1137/S106482750139738X.